Article

Anomalous Concentration Dependence of Surface Tension and Concentration-Concentration Correlation Functions of Binary Non-Electrolyte Solutions

Carlo Carbone [1], Eduardo Guzmán [1,2] and Ramón G. Rubio [1,*]

1 Departamento de Química Física, Facultad de Ciencias Químicas, Universidad Complutense de Madrid, Ciudad Universitaria s/n, 28040 Madrid, Spain
2 Instituto Pluridisciplinar, Universidad Complutense de Madrid, Paseo de Juan XXIII 1, 28040 Madrid, Spain
* Correspondence: rgrubio@quim.ucm.es; Tel.: +34-91-3944123

Abstract: The concentration dependence of the surface tension of several binary mixtures of non-electrolytes has been measured at 298.15 K. The mixtures have been chosen since they presented a so-called "W-shape" concentration dependence of the excess constant pressure heat capacity and high values of the concentration-concentration correlation function. This behavior was interpreted in terms of the existence of anomalously high concentration fluctuations that resemble those existing in the proximities of critical points. However, no liquid-liquid phase separation has been found in any of these mixtures over a wide temperature range. In this work, we have extended these studies to the liquid-air interfacial properties. The results show that the concentration dependence of the surface tension shows a plateau and the mixing surface tension presents a "W-shape" behavior. To the best of our knowledge, this is the first time that this behavior is reported. The weak anomalies of the surface tension near a liquid-liquid critical point suggest that the results obtained cannot be considered far-from-critical effects. The usual approach of substituting the activity by the concentration in the Gibbs equation for the relative surface concentration has been found to lead to large errors and the mixtures to have a fuzzy and thick liquid/vapor interface.

Keywords: binary mixtures; critical point; fluctuations; non-electrolytes; surface tension

1. Introduction

In the last few years, several works showed that the excess constant pressure heat capacity, C_P^E, of some binary mixtures of non-electrolytes presented an anomalous concentration dependence [1–3]. More specifically, this dependence had a more or less pronounced W-shape. The molecules of the studied mixtures did not have any chemical structural correlation. A very extensive description of the fluctuation theory of mixtures and its consequences on the thermodynamic properties of liquid mixtures is provided by Matteoli and Mansoori [4]. Depolarized light scattering experiments performed by Rubio et al. [5] allowed for the determination of the so-called concentration-concentration correlation function, S_{cc}, which is the zero-wave vector limit of the structure factor. The authors pointed out that, for these binary mixtures, S_{cc} took values significantly higher than those corresponding to an ideal mixture, thus indicating that the concentration fluctuations were high. Therefore, at the molecular level, the composition was clearly non-random, thus differing from the overall one. Experimental evidence of the difference between bulk and local concentrations has been provided by different authors using spectroscopic methods [6–8], as well as computer simulations [9–11] and theoretical calculations [12–15]. Notably, S_{cc} is the inverse darken stability [16–19] and is closely related to the osmotic compressibility, $\left(\frac{\partial \mu_i}{\partial x_i}\right)_{T,P}$, with μ_i being the chemical potential. It is well known that $S_{cc}(0)$ values much higher than the one for ideal mixtures (max. $S_{cc}(0) = 0.25$ for $x = 0.5$) are typical of the

systems near a critical point. However, the decrease in the temperature of the studied mixtures did not lead to any phase separation; therefore, far-from-critical effects are difficult to be considered for justifying the results found.

It is well known that in binary mixtures the osmotic compressibility gives the excess surface concentration of component i at the vapor/liquid interface. In most cases reported in the literature, an ideal behavior is defined as $\mu_i(T, P) = \mu_i^0(T, P = 1\,\text{bar}) + RT \ln x_i$, with x_i being the mole fraction of component i. However, Coto et al. [20] have shown that assuming an ideal behavior to calculate the osmotic compressibility may be inadequate for calculating surface relative adsorption, $\Gamma_{2,1}$, which is also observed for dilute water-alcohol mixtures. Using small angle neutron scattering, Almasi et al. [21] have shown that small errors in the excess Gibbs energy, G^E, may lead to large errors in $\left(\frac{\partial \mu_2}{\partial x_2} \right)_T$. Ritacco et al. [22,23] reported that aqueous trisiloxane solutions are an example of this problem from ellipsometry measurements. Similar conclusions were obtained from Llamas et al. [24,25] by combining surface tension and neutron reflectometry measurements.

Concentration fluctuations have been found to have strong consequences on other thermodynamic properties, even relatively far from any critical point, and for mixtures in which strong interactions, e.g., hydrogen bonds, exist. An example is the mixture that shows W-shape C_p^E curves. Similar conclusions have been reached for aqueous solutions [26–34].

The adsorbed amount of component 2 relative to component 1, $\Gamma_{2,1}$, is directly related to the composition dependence of the surface tension and chemical potential, μ_2, through the Gibbs equation:

$$\Gamma_{2,1} = -\left(\frac{\partial \gamma}{\partial \mu_2} \right)_T. \tag{1}$$

The difficulty in precisely calculating the chemical potential from experimental data, has most frequently led researchers to assume an ideal behavior for the mixtures, thus Equation (1) can be rewritten as [35]:

$$\Gamma_{2,1} = -\frac{1}{RT} x_2 \left(\frac{\partial \gamma}{\partial x_2} \right)_T. \tag{2}$$

In general, it is clear that Equation (2) cannot be applied to concentrated mixtures, such as those studied in this work. Despite some approximate methods that have been proposed for calculating μ_2 [36], we have preferred to calculate $\Gamma_{2,1}$ using experimental data, thus not relying on any theoretical approximation.

More direct methods for measuring $\Gamma_{2,1}$ have been described in the literature. Ellipsometry [37,38] and neutron or X-ray reflectometry [39–43], as well as radiative decomposition of tritium-doped molecules [44] have provided reliable values of $\Gamma_{2,1}$ for binary mixtures, including dilute solutions of soluble surfactants. However, in some cases, e.g., for ellipsometry or reflectometry, it is necessary to assume the validity of a structural model for the interface, and then to fit the experimental data to the predictions of the model. Moreover, in the case of ellipsometry, the small difference in the refractive indexes of the components in each mixture does not allow one to obtain reliable values of the surface thickness.

Concentration fluctuations, as measured by the concentration-concentration correlation functions (zero wave-vector structure factor), are directly related to the osmotic compressibility by

$$S_{cc}^{-1}(0) = \frac{1}{RTx_1 x_2} \left(\frac{\partial \mu_2}{\partial \ln x_2} \right)_T \tag{3}$$

A brief description of the relationship of $S_{cc}(0)$ with the integral theory of fluids is provided in Appendix A.

It is well known that $S_{cc}(0)$ diverges close to the critical points, whereas it takes a simple expression for ideal solutions, $S_{cc}(0) = x_1 \cdot x_2$. The values of $S_{cc}(0)$ for the studied systems have been obtained from depolarized light scattering experiments, as described in detail in Appendix.

The overall goal of this manuscript is to study whether the systems that presented W-shape C_P^E curves also show an anomalous behavior on the concentration dependence of the surface tension. The reason for this possibility is that, in equilibrium, μ_i (bulk) = μ_i (interface); therefore, strong concentration fluctuations in the bulk might affect the surface properties. Furthermore, we will discuss the excess consequences for the relative surface concentration behavior.

2. Materials and Methods

All solvents used in this work were purchased from Sigma-Aldrich (Saint Louis, MO, USA) and were of the maximum purity available, always exceeding 99.8 wt%. However, in the case of chloronaphtalene, the commercial purity was below 99 wt% in order that it was purified by five melting-thawing cycles until no impurities were detected by gas chromatography. Moreover, constant surface tension and density were observed after two consecutive cycles.

The surface tension was measured using three different tensiometers: Pendant drop, Wilhelmy plate, and de Nouy ring. The first was home made and the ADSA analysis was used for the analysis of the drop profile, as in previous works [24,25]. The Wilhelmy plate measurements were performed using a Nima model 702 Langmuir balance (Biolin, Göteborg, Sweden) and the ring experiments were carried out in a Krüs K-10 tensiometer (Krüs GmbH, Hamburg, Germany). Since the presence of impurities may lead to a time dependent surface tension due to the adsorption of the impurities, we have performed adsorption kinetic measurements for three mole fractions, 0.2, 0.5, and 0.8, for 2-butanone + n-decane, as well as chloronaphtalene + 2,2,4-trimethylpentane. The equilibration time in the plate and ring tensiometers were less than 2 min when each component has been thermostated prior to mixing. This is in accordance with the low viscosity and high diffusion coefficients of the solvents. Our techniques do not allow us to follow a sufficiently detailed kinetic measurement for these short stabilization times. Moving barrier measurements using a Langmuir balance induced a 400% reduction in the initial area. No change in the surface tension was detected within the experimental uncertainty. Therefore, we can conclude that the compounds were sufficiently pure for the surface tension experiments.

The density measurements were carried out using an Anton Paar vibrating tube tensiometer DMA 4200-M (Anton Paar, Graz, Austria) with a precision of 3×10^{-5} g/cm^{-3}.

The light scattering experiments were performed using an ALV/CGS-03 precision photogoniometer that uses a ALV-5000 correlator and a Glass-Thompson polarizer (ALV-Laser Vertriebsgesellschaft GmbH, Langen, Germany). This equipment was used in previous works [45] and includes a Coherent laser beam (Coherent Inc., Santa Clara, CA, USA) working at 532 nm. The refractive index was measured using a Carl-Zeiss refractometer (Jena, Germany) at 546 nm, with a precision of 10^{-5} units. Since it is important to obtain reliable values of $S_{cc}(0)$, independent values of $\left(\frac{\partial n}{\partial x_2}\right)$ were obtained using a BI-DNDC differential refractometer (Brookhaven Instrument Corporation, Holtsville, NY, USA) with a precision of 10^{-3} units.

Milli-Q water was used for cleansing with a resistivity higher than 18 MΩ·cm and an organic material content lower than 6 ppm. The glassware was cleaned with piranha solution (caution: Piranha solutions are dangerous), then thoroughly rinsed with pure water and dried in a vacuum oven.

3. Results and Discussion

Figure 1 shows the mole fraction dependence of the surface tension for the different studied mixtures. It is important to note the existence of a more or less extended pseudoplateau, which to date, has not been described in the literature. Even for mixtures close to their lower critical solution temperature (LCST), the pseudoplateau is not more pronounced [46]. Nevertheless, it must be noted that the experimental γ vs. X data do not show any maximum, minimum, or inflection point where $\left(\frac{\partial \gamma}{\partial x}\right)_{T,P} = 0$, thus leading to $\Gamma_{2,1} = 0$.

This situation is found, e.g., in the case of aneotropic points, and has been discussed in detail in a book by Lyklema on binary mixtures of simpler compounds [47]. For completeness, we have included the results for the system methanol + methy-tertbutyl-ether (MTBE), in which no pseudoplateau is observed. Figure 1d shows that for the mixtures containing 1,2-dibromoethane, the plateau shifts to lower values of x_1 as the chain length of the hydrocarbon decreases. On the other hand, the decrease in T shifts the pseudoplateau toward higher values of x1. Furthermore, as an example, Figure 1e shows that by lowering the temperatures of the mixtures no phase separation was found, as for any of the other mixtures. It has not been possible to describe the behavior observed using any of the available theoretical models within the experimental precision. The shape of the isotherms is similar to the type 2 gas adsorption isotherms (BET model) if $\gamma - \gamma_2$ is plotted. Using this model as an empirical equation no good fit was obtained, even by using a maximum likelihood algorithm that includes the uncertainty in both dependent and independent variables [48]. Therefore, a pure empirical fitting approach has been used, while taking care that no numerical artifacts were introduced in the calculation of the derivative of γ vs. X.
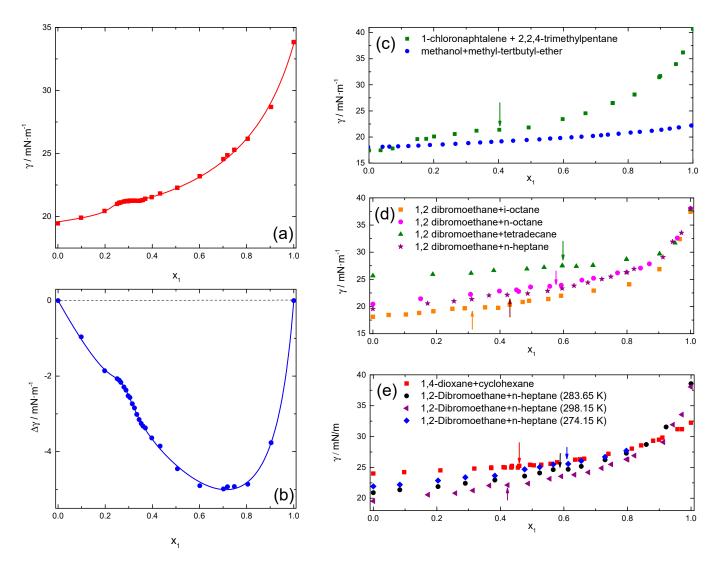

Figure 1. Composition of dependences of the surface tension (**a**) and mixing surface tension, $\Delta\gamma$, (**b**) at 298.15 K for 1,4-dichlorobutane + n-heptane mixtures. Symbols are the experimental results and curves that fit into Equation (4) with n = m = 3. In panels from (**c**–**e**), the composition dependences of the surface tension for the different studied systems are displayed. The insets identify the mixtures and the temperatures of the measurements, 298.15 K, unless the other value is specified. The arrows indicate the positions of the pseudo plateaus.

In order to calculate $\left(\frac{\partial \gamma}{\partial x_2}\right)_{T,P}$ with sufficiently high precision, both the surface tension and the mixing surface tension, $\Delta \gamma = \gamma - X_1 \cdot \gamma_1 - X_2 \cdot \gamma_2$, have been fitted to Padé approximants:

$$Y = \Lambda \frac{\sum_{i=0}^{n} A_i x_1^i}{1 + \sum_{j=1}^{m} B_j x_1^j},. \tag{4}$$

where A_i and B_i are fitting parameters, $\Lambda = 1$ for the surface tension, γ, and $\Lambda = x_{1 \times 2}$ for the mixing surface tension, $\Delta \gamma$. Maximum values of 3 for n and m have been used for the sum of Equation (4), while ensuring that the uncertainties of the parameters used were less than 5%. For example, Figure 1a,b shows the experimental results and the corresponding fitted curves for the 1,4-dichlorobutane + n-heptane system, in which the plateau is more visible and has been experimentally mapped in more detail. It is clear that the fits are very good, and lead to randomly distributed residuals (not shown). For completeness, it is convenient to indicate that the experimental uncertainty on $S_{cc}(0)$ is about 3%, although it depends slightly on the difference in the refractive index of the compounds and their polarizability tensors.

As explained in Appendix A:

$$S_{cc}^{-1}(0) = \frac{1}{RTx_1 x_2} \left(\frac{\partial \mu_2}{\partial \ln x_2}\right)_T, \tag{5}$$

thus leading to

$$\Gamma_{2,1}(x_2) = -x_1 \frac{\left(\frac{\partial \gamma}{\partial x_2}\right)_{T,P}}{S_{cc}(x_2)}. \tag{6}$$

Figure 2 shows the composition dependence of $S_{cc}(0)$ for the different studied mixtures. Some of the results were already published in a previous paper [5]; however, in order to have a more precise value for $\Gamma_{2,1}$, we have performed additional experiments for better interpolation at the concentrations measured for γ. In all cases, it can be observed that the values are noticeably higher than the ideal mixture. Indeed, in some cases, the maxima of the curves are one order of magnitude higher, which as discussed below, has drastic consequences on the excess surface calculations.
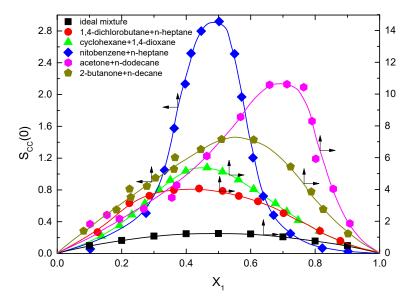

Figure 2. Composition dependence of the concentration-concentration correlation function at 298.15 K. The dashed-dotted line corresponds to an ideal mixture. Notice that some of the curves refer to the left ordinate axis, while the others refer to the right axis. Some of the data shown have been reproduced with permission from our previous publication [5].

Combining the values of $\left(\frac{\partial\gamma}{\partial x_2}\right)_{T,P}$ calculated from the experimental results and Equation (6), the excess surface concentration, $\Gamma_{2,1}$, can be calculated from the experimental results. Notably, since the $\left(\frac{\partial\gamma}{\partial x_2}\right)_{T,P}$ is an experimental result independent of whether the mixture has been considered ideal or real, the ratio $\frac{\Gamma_{2,1}^{real}(x_2)}{\Gamma_{2,1}^{ideal}(x_2)} = \frac{S_{cc}^{ideal}(x_2)}{S_{cc}^{real}(x_2)}$ will give a direct information of how far the ideal mixture assumption is reliable. Since $S_{cc}(0) = x_1 \cdot x_2$ for an ideal mixture, the experimental values shown in Figure 2 clearly point out that for the studied systems in this work, this approximation is not acceptable. An immediate conclusion is that the excess surface adsorption for these mixtures is smaller than the ideal mixtures except for the nitrobenzene + n-heptane in the high x_1 region, as shown in Figure 3. A possible explanation is that the high values of the concentration-concentration correlation function indicate that the concentration which is very close to a molecule of type 2, $X_{2,local}$, is quite different from the average macroscopic value, X_2. However, $X_{2,local}$ around one molecule of type 2 is not exactly the same as around another molecule of the same type at a different position at the same time. Ultimately, of course, the average value of $X_{2,local}$ for all the molecules of type 2 has to be equal to the average value of X_2.
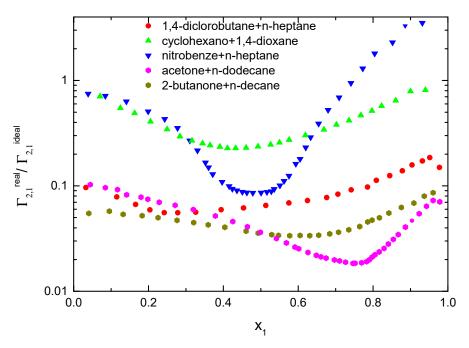

Figure 3. Ratio of the relative surface concentration, $\Gamma_{2,1}$, for real and ideal mixtures.

4. Conclusions

The surface tension and the concentration-concentration has been measured for non-electrolyte binary mixtures that presented a "W-shape" C_P^E-composition dependence. An anomalous concentration dependence has been found both for the surface tension and the mixing surface tension. The first shows a plateau at intermediate compositions, and the mixing surface tension shows a marked shoulder in the plateau region. The concentration fluctuations have been obtained from depolarized light scattering experiments. The values obtained are well above the values corresponding to the ideal mixture. The combination of the two types of results clearly shows that the most usual approximation for calculating the relative excess surface concentration, in which the activities of the two components are substituted by mole fractions, is not acceptable. Indeed, the ratio between the values of the excess concentration calculated using the ideal mixture approximation and those rigorously calculated can be up to two orders of magnitude for the studied mixtures. Considering the high values of the concentration-concentration correlation function for the mixtures,

associated with strong concentration fluctuations, these results can be associated with a high thickness of the liquid/vapor interface.

Appendix A

The relationships between the osmotic compressibility and the concentration-concentration correlation functions are based on the integral theory of fluids derived by Kirkwood and Buff [49]. In the case of binary mixtures, the structure has been better discussed in terms of the partial structure factors, $a_{ij}\left(\vec{q}\right)$, where $\vec{q}$ is the wave-vector, and i and j refer to the two types of molecules. The partial structure factors are defined as

$$a_{ij}\left(\vec{q}\right) = 1 + \rho \int_0^\infty \left[g_{ij}(r) - 1\right] \exp\left(i \cdot \vec{q} \cdot \vec{r}\right) d\vec{r}, \tag{A1}$$

where $g_{ij}(r)$ is the radial distribution function of molecules i and j, $\vec{r}$ is the vector joining the center of the two molecules, and ρ is the density. In the exponential, $i = \sqrt{-1}$.

The long-wave limits of the partial structure factors, q→∞, are directly related to the so-called Kirkwood-Buff integrals [49,50]

$$G_{ij} = \int_0^\infty \left[g_{ij}(r) - 1\right] \cdot 4\pi r^2 dr, \tag{A2}$$

which are related to the osmotic compressibility [51] through

$$G_{ij} = RT\kappa_T - \frac{V_i \cdot V_j}{D \cdot V} \; ; \; G_{ii} = G_{ij} + \frac{\left[\frac{V_j}{D} - V\right]}{X_i}, \tag{A3}$$

where V_i and V_j denote the molar volume of component i and j, respectively, V is the molar volume of the mixture, κ_T is the isothermal compressibility, and D is given by

$$D = \frac{X_1 X_2}{S_{cc}(0)} = \frac{X_i}{RT}\left(\frac{\partial \mu_i}{\partial X_i}\right). \tag{A4}$$

Appendix B

$S_{cc}(0)$ is the form factor S(q) in the limit of zero wave vector, q = 0, thus giving long-range information of system fluctuations, which in the case of mixtures, correspond

to concentration fluctuations, and thus on the local concentrations. Therefore, from the macroscopic point-of-view, $S_{cc}(0)$ is directly related to the osmotic compressibility of the system. It is known that the long-range fluctuations can be measured from diffraction experiments, typically using synchrotron radiation or depolarized light scattering.

The excess surface concentration at the air liquid/vapor interface is directly related to the osmotic compressibility by

$$\Gamma_{2,1}(x_2) = -\frac{1}{RT}\frac{\left(\frac{\partial\gamma}{\partial x_2}\right)_{T,P}}{\left(\frac{\partial\ln\mu_2}{\partial x_2}\right)_{T,P}} \Rightarrow \Gamma_{2,1}(x_2) = -x_1\frac{\left(\frac{\partial\gamma}{\partial x_2}\right)_{T,P}}{S_{cc}(x_2)}, \tag{A5}$$

where γ is the surface tension, x_2 is the molar fraction of component 2, a_2 is its activity, which is related to its chemical potential by $\mu_2(x_2, T, P) = \mu_2^0 + RT\ln a_2(x_2, T, P)$, and μ_2^0 is the standard chemical potential of component 2. The numerator of Equation (A1) only requires precise measurements of the γ composition dependence, which is not difficult. However, the denominator is more complicated from the experimental point-of-view, as explained below.

The Gibbs-Duhem equation allows one to write

$$\left[\frac{\partial\ln x_2}{\partial\left(\frac{\mu_2}{RT}\right)}\right]_{T,P} = -\frac{x_1}{x_2}\left[\frac{\partial\left(\frac{\mu_1}{RT}\right)}{\partial\ln x_1}\right]_{T,P}. \tag{A6}$$

the left-hand side of Equation (A2) is related to the Rayleigh ratio by

$$\left[\frac{\partial\ln x_2}{\partial\left(\frac{\mu_2}{RT}\right)}\right]_{T,P} = \frac{R_c}{R_{id}}, \tag{A7}$$

with R_c being defined by

$$R_i = R - R_c - R^*, \tag{A8}$$

where R is the Rayleigh ratio for non-polarized incident light, and was obtained from the scattered intensity, I, using toluene as reference according to $R = R_T\frac{I}{I_T}\left(\frac{n}{n_T}\right)^2$, the unsubscribed magnitudes referring to the mixture, and the ones with subscript T to the toluene n are the refractive index, R, which has isotropic and anisotropic contributions, R_i and R_a, respectively. In our case, R_i is the contribution that matters, and can be calculated through $R_i = R\frac{6-7\rho_u}{6+6\rho_u}$, with ρ_u being the depolarization factor, $\rho_u = \frac{I_H}{I_V}$, where I_H and I_V are the scattered intensities of horizontally and vertically polarized laser beams, respectively.

For binary liquid mixtures, R_i contains three contributions $R_i = R_d + R_c + R^*$, where R_d and R_c are due to separate fluctuations of the density and concentration, respectively. R* gives the correlation between the two types of fluctuations by

$$R_d = \frac{\pi^2}{2\lambda_0^4}k_BT\kappa_T\left[\rho\left(\frac{\partial\varepsilon}{\partial\rho}\right)\right]^2$$

$$R_c = \frac{\pi^2}{2\lambda_0^4}k_BTV\frac{\left(\frac{\partial\varepsilon}{\partial x_2}\right)_T^2}{\left(\frac{\partial\mu_2}{\partial x_2}\right)_T} \tag{A9}$$

$$R^* = \frac{\pi^2}{2\lambda_0^4}k_BT\kappa_T\rho\left(\frac{\partial\varepsilon}{\partial\rho}\right)_{x,T}x_1x_2\left(\frac{\partial\varepsilon}{\partial x_2}\right)_{T'}$$

where λ_0 denotes the laser wavelength in the vacuum, k_B is the Boltzmann constant, ρ is the density, κ_T is the isothermal compressibility, V is the molar volume, and ε is the relative dielectric permittivity given, for infinite wavelength, by $\varepsilon = n_2$.

According to Segudovic and Dezelic [52], R* can be expressed, in a first approximation, as

$$R^* = \frac{\pi^2}{2\lambda_0^4} k_B T \kappa_T \rho \left(\frac{\partial \varepsilon}{\partial \rho} \right)_{x,T} x_1 x_2 \left(\frac{\partial \varepsilon}{\partial x_2} \right)_T. \tag{A10}$$

Simplifying the previous equations for ideal mixtures, $a_2 = x_2$, the Rayleigh ratio is given by

$$R_{id} = \frac{\pi^2}{2\lambda_0^4} x_1 x_2 \frac{V}{N_A} \left(\frac{\partial \varepsilon}{\partial x_2} \right)^2, \tag{A11}$$

where N_A is Avogadro's number. Therefore, for a real mixture, R_c can be expressed as $R_c = R_{id} \left[\frac{\partial \left(\frac{\mu_2}{RT} \right)}{\partial \ln x_2} \right]^{-1}_{T,P}$, which combined with Equations (A4) and (A7) allow one to obtain $\partial \left(\frac{\mu_2}{RT} \right)$ and, therefore, $S_{cc}(0)$.

For the density dependence of the relative permittivity one can use the Eykman equation, that assumes $\varepsilon \approx n^2$, which is a high-frequency approximation valid for our experiments, e.g., see Johnson and Smith [53]:

$$\rho \left(\frac{\partial \varepsilon}{\partial \rho} \right)_{x,T} = \frac{2n(n^2 - 1)(n + 0.4)}{n^2 + 1} + 0.8n. \tag{A12}$$

References

1. Lainez, A.; Roux-Desgranges, G.; Grolier, J.P.E.; Wilhelm, E. Mixtures of alkanes with polar molecules showing internal rotation: An unusual composition dependence of CpE of 1,2-dichloroethane + an n-alkane. *Fluid Phase Equilibria* **1985**, *20*, 47–56. [CrossRef]
2. Saint Victor, M.-E.; Patterson, D. The W-shaped concentration dependence of CpE and solution non-randomness: Systems approaching the UCST. *Thermochim. Acta* **1990**, *159*, 177–185. [CrossRef]
3. Saint-Victor, M.-E.; Patterson, D. The w-shape concentration dependence of CEp and solution non-randomness: Ketones + normal and branched alkanes. *Fluid Phase Equilibria* **1987**, *35*, 237–252. [CrossRef]
4. Matteoli, E.; Mansoori, G.A. (Eds.) *Fluctuation Theory of Mixtures*; Taylor & Francis: Boca Raton, FL, USA, 1990.
5. Rubio, R.G.; Cáceres, M.; Masegosa, R.M.; Andreolli-Ball, L.; Costas, M.; Patterson, D. Mixtures with "w-Shape" C^Ep curves. A light scattering study. *Ber. Bunsenges. Phys. Chem.* **1989**, *93*, 48–56. [CrossRef]
6. Mello, C.; Mello, T.; Sevéri, E.; Coelho, L.; Ribeiro, D.; Marangoni, A.; Poppi, R.J.; Noda, I. Microstructures formation in a seemingly ideal homogeneous mixture of ethanol and methanol: An experimental evidence and two-dimensional correlation spectroscopy approach. *J. Chem. Phys.* **2009**, *131*, 084501. [CrossRef]
7. Phillips, D.J.; Brennecke, J.F. Spectroscopic measurement of local compositions in binary liquid solvents and comparison to the NRTL equation. *Ind. Eng. Chem. Res.* **1993**, *32*, 943–951. [CrossRef]
8. Shulgin, I.L.; Ruckenstein, E. Excess around a central molecule with application to binary mixtures. *Phys. Chem. Chem. Phys.* **2008**, *10*, 1097–1105. [CrossRef]
9. Požar, M.; Perera, A. Evolution of the micro-structure of aqueous alcohol mixtures with cooling: A computer simulation study. *J. Mol. Liquids* **2017**, *248*, 602–609. [CrossRef]
10. Sarkar, S.; Maity, A.; Chakrabarti, R. Microscopic structural features of water in aqueous–reline mixtures of varying compositions. *Phys. Chem. Chem. Phys.* **2021**, *23*, 3779–3793. [CrossRef]
11. Perera, A.; Kežić, B. Fluctuations and micro-heterogeneity in mixtures of complex liquids. *Faraday Discuss.* **2013**, *167*, 145–158. [CrossRef]
12. Chen, H.-F.; Li, J.-T.; Gu, F.; Wang, H.-J. Kirkwood-Buff integrals for hard-core Yukawa fluids. *Eur. Phys. J. E* **2017**, *40*, 93. [CrossRef]
13. Bentenitis, N.; Cox, N.R.; Smith, P.E. A Kirkwood−Buff Derived Force Field for Thiols, Sulfides, and Disulfides. *J. Phys. Chem. B* **2009**, *113*, 12306–12315. [CrossRef]
14. Debenedetti, P.G. The statistical mechanical theory of concentration fluctuations in mixtures. *J. Chem. Phys.* **1987**, *87*, 1256–1260. [CrossRef]
15. Shimizu, S.; Matubayasi, N. Statistical thermodynamic foundation for mesoscale aggregation in ternary mixtures. *Phys. Chem. Chem. Phys.* **2018**, *20*, 13777–13784. [CrossRef]
16. Nishikawa, K.; Hayashi, H.; Iijima, T. Temperature Dependence of the Concentration Fluctuation, the Kirkwood-Buff Parameters, and the Correlation Length of fed-Butyl Alcohol and Water Mixtures Studied by Small-Angle X-ray Scattering. *J. Phys. Chem.* **1989**, *93*, 6559–6565. [CrossRef]
17. Hayashi, H.; Nishikawa, K.; Iijima, T. Small-Angle X-ray Scattering Study of Fluctuations in 1-Propanol-Water and 2-Propanol-Water Systems. *J. Phys. Chem.* **1990**, *90*, 8334–8338. [CrossRef]

18. Hayashi, H.; Morita, T.; Nishikawa, K. Interpretation of correlation length by small-angle X-ray scattering experiments on fluids near critical point. *Chem. Phys. Lett.* **2009**, *471*, 249–252. [CrossRef]

19. Tsuchiya, Y. Elucidation of structural changes and concentration fluctuations in binary mixtures using new thermodynamic relations. *J. Phys. Condens. Matter* **1999**, *11*, 593. [CrossRef]

20. Coto, B.; Mößner, F.; Pando, C.; Rubio, R.G.; Renuncio, J.A.R. Bulk and surface properties for the methanol–1,1-dimethylpropyl methyl ether and methanol–1,1-dimethylethyl methyl ether systems. *J. Chem. Soc. Faraday Trans.* **1996**, *92*, 4435–4440. [CrossRef]

21. Almasi, M.; Khodamoradpoor, M. Study of molecular interactions in binary mixtures by molecular diffusion, thermal diffusion, Soret effect, and separation ratio. *J. Mol. Liquids* **2021**, *335*, 116545. [CrossRef]

22. Ritacco, H.A.; Fainerman, V.B.; Ortega, F.; Rubio, R.G.; Ivanova, N.; Starov, V.M. Equilibrium and dynamic surface properties of trisiloxane aqueous solutions. Part 2. Theory and comparison with experiment. *Colloids Surf. A* **2010**, *365*, 204–209. [CrossRef]

23. Ritacco, H.A.; Ortega, F.; Rubio, R.G.; Ivanova, N.; Starov, V.M. Equilibrium and dynamic surface properties of trisiloxane aqueous solutions: Part 1. Experimental results. *Colloids Surf. A* **2010**, *365*, 199–203. [CrossRef]

24. Llamas, S.; Fernández-Peña, L.; Akanno, A.; Guzmán, E.; Ortega, V.; Ortega, F.; Csaky, A.G.; Campbell, R.A.; Rubio, R.G. Towards understanding the behavior of polyelectrolyte–surfactant mixtures at the water/vapor interface closer to technologically-relevant conditions. *Phys. Chem. Chem. Phys.* **2018**, *20*, 1395–1407. [CrossRef]

25. Llamas, S.; Guzmán, E.; Akanno, A.; Fernández-Peña, L.; Ortega, F.; Campbell, R.A.; Miller, R.; Rubio, R.G. Study of the Liquid/Vapor Interfacial Properties of Concentrated Polyelectrolyte–Surfactant Mixtures Using Surface Tensiometry and Neutron Reflectometry: Equilibrium, Adsorption Kinetics, and Dilational Rheology. *J. Phys. Chem. C* **2018**, *122*, 4419–4427. [CrossRef]

26. Pandey, J.D.; Verma, R. Inversion of the Kirkwood–Buff theory of solutions: Application to binary systems. *Chem. Phys.* **2001**, *270*, 429–438. [CrossRef]

27. Blanco, M.A.; Sahin, E.; Li, Y.; Roberts, C.J. Reexamining protein-protein and protein-solvent interactions from Kirkwood-Buff analysis of light scattering in multi-component solutions. *J. Chem. Phys.* **2011**, *134*, 225103. [CrossRef]

28. Matteoli, E.; Lepori, L. Kirkwood–Buff integrals and preferential solvation in ternary non-electrolyte mixtures. *J. Chem. Soc. Faraday Trans.* **1995**, *91*, 431–436. [CrossRef]

29. Matteoli, E.; Mansoori, G.A. A simple expression for radial distribution functions of pure fluids and mixtures. *J. Chem. Phys.* **1995**, *103*, 4672–4677. [CrossRef]

30. Matteoli, E. A Study on Kirkwood−Buff Integrals and Preferential Solvation in Mixtures with Small Deviations from Ideality and/or with Size Mismatch of Components. Importance of a Proper Reference System. *J. Phys. Chem. B* **1997**, *101*, 9800–9810. [CrossRef]

31. Wilcox, D.S.; Rankin, B.M.; Ben-Amotz, D. Distinguishing aggregation from random mixing in aqueous t-butyl alcohol solutions. *Faraday Discuss.* **2013**, *167*, 177–190. [CrossRef]

32. Chakraborty, S.; Sehanobish, E.; Sarkar, M. A traditional painkiller as a probe for microheterogeneity in 1-propanol–water mixtures. *Chem. Phys. Lett.* **2010**, *501*, 118–122. [CrossRef]

33. Oh, K.-I.; Baiz, C.R. Molecular heterogeneity in aqueous cosolvent systems. *J. Chem. Phys.* **2020**, *152*, 190901. [CrossRef] [PubMed]

34. Marcus, Y. Preferential solvation in mixed solvents. Part 5.—Binary mixtures of water and organic solvents. *J. Chem. Soc. Faraday Trans.* **1990**, *86*, 2215–2224. [CrossRef]

35. Ramírez-Verduzco, L.F.; Romero-Martínez, A.; Trejo, A. Prediction of the surface tension, surface concentration, and the relative Gibbs adsorption isotherm of binary liquid systems. *Fluid Phase Equilibria* **2006**, *246*, 119–130. [CrossRef]

36. Bagheri, A.; Rafati, A.A.; Tajani, A.A.; Borujeni, A.R.A.; Hajian, A. Prediction of the Surface Tension, Surface Concentration and the Relative Gibbs Adsorption Isotherm of Non-ideal Binary Liquid Mixtures. *J. Solut. Chem.* **2013**, *42*, 2071–2086. [CrossRef]

37. Heidel, B.; Findenegg, G.H. Ellipsometric study of the surface of a binary liquid mixture near a critical solution point. *J. Phys. Chem.* **1984**, *88*, 6575–6579. [CrossRef]

38. Privat, M.; Bennes, R.; Tronel-Peyroz, E.; Douillard, J.-M. Ellipsometry and adsorption: The determination of isotherms and the adsorbed layer thickness and fluctuations of the composition in the liquid-vapor interface. *J. Colloid Interface Sci.* **1988**, *121*, 198–207. [CrossRef]

39. Subramanian, D.; Boughter, C.T.; Klauda, J.B.; Hammouda, B.; Anisimov, M.A. Mesoscale inhomogeneities in aqueous solutions of small amphiphilic molecules. *Faraday Discuss.* **2013**, *167*, 217–238. [CrossRef]

40. Shulgin, I.; Ruckenstein, E. Kirkwood−Buff Integrals in Aqueous Alcohol Systems: Aggregation, Correlation Volume, and Local Composition. *J. Phys. Chem. B* **1999**, *103*, 872–877. [CrossRef]

41. Nishikawa, K.; Morita, T. Small-Angle X-ray-Scattering Study of Supercritical Trifluoromethane. *J. Phys. Chem. B* **1997**, *101*, 1413–1418. [CrossRef]

42. Morita, T.; Nishikawa, K. Fluctuations in density and concentration of methanol–water mixtures at 7 MPa and 373, 423 K studied by small-angle X-ray scattering. *Chem. Phys. Lett.* **2004**, *389*, 29–33. [CrossRef]

43. Nishikawa, K.; Kasahara, Y.; Ichioka, T. Inhomogeneity of Mixing in Acetonitrile Aqueous Solution Studied by Small-Angle X-ray Scattering. *J. Phys. Chem. B* **2002**, *106*, 693–700. [CrossRef]

44. Kopf, S.; Bourriquen, F.; Li, W.; Neumann, H.; Junge, K.; Beller, M. Recent Developments for the Deuterium and Tritium Labeling of Organic Molecules. *Chem. Rev.* **2022**, *122*, 6634–6718. [CrossRef] [PubMed]

45. Hernández, M.a.P.; Ortega, F.; Rubio, R.G. Crossover critical phenomena in an aqueous electrolyte solution: Light scattering, density and viscosity of the 3-methylpyridine+water+NaBr system. *J. Chem. Phys.* **2003**, *119*, 4428–4436. [CrossRef]

46. Díez-Pascual, A.; Ortega, F.; Crespo-Colín, A.; Compostizo, A.; Monroy, F.; Rubio, R.G. Concentration Fluctuations and Surface Adsorption in Hydrogen-Bonded Mixtures. *J. Phys. Chem. B* **2004**, *108*, 10019–10024. [CrossRef]
47. Lyklema, J. *Fundamentals of Interface and Colloid Science*; Academic Press: Cambridge, MA, USA, 2000.
48. Rubio, R.G.; Renuncio, J.A.R.; Peña, M.D. Regression of vapor-liquid equilibrium data based on application of the maximum-likelihood principle. *Fluid Phase Equilibria* **1983**, *12*, 217–234. [CrossRef]
49. Kirkwood, J.G.; Buff, F.P. The Statistical Mechanical Theory of Solutions. I. *J. Phys. Chem.* **1951**, *19*, 774–777. [CrossRef]
50. McQuarrie, D.A. *Statistical Mechanics*; Harper & Row: New York, NY, USA, 1973.
51. Gray, C.G.; Gubbins, K.E. *Theory of Molecular Fluids*; Oxfort University Press: London, UK, 1984.
52. Segudovic, N.; Dezelic, G. Light Scattering in Binary Liquid Mixtures. I. Isotropic Scattering. *Croat. Chem. Acta* **1973**, *45*, 385–406.
53. Johnson, B.L.; Smith, J. *Light Scattering from Polymer Solutions*; Huglin, M.B., Ed.; Academic Press: New York, NY, USA, 1972.